Carpathian Journal of Earth and Environmental Sciences February 2024, Vol. 19, No. 1, p. 169 – 178; DOI:10.26471/cjees/2024/019/288

WASHING OF HEAVY METAL-CONTAMINATED SOILS USING PYOVERDINE EXTRACTED FROM PLANT GROWTH-PROMOTING BACTERIA *PSEUDOMONAS LACTIS* AND *P. ATACAMENSIS*

Hibat Errahmen MAZARI[1*], Amina MELIANI[2], Samir BERKAT[1], Samia ALIANE [1], Rachid DJIBAOUI[3], & Kaddour BOUDEROUA[4]

[1]*Geo-environment and space development laboratory (LGEDE), Faculty of Nature and Life Science, University of Mustapha Stambouli, Mascara, Algeria*

[2]*Department of Biology, Faculty of Nature and Life Science, University Mustapha Stambouli, Mascara, Algeria*

[3]*Laboratory of Microbiology and Plant Biology, Faculty of Nature and Life Science, University of Abdlhamid Ibn Badis, Mostaganem, Algeria*

[4]*Laboratory of Biotechnology Applied to Agriculture and Environmental Preservation in Higher School of Agronomy "Mohamed El Amjed Ben Abdel Malek", Hall Technology Kharouba, Mostaganem-Algeria.*

**Correspondence: hibaterrahmen.mazari@univ-mascara.dz*

Abstract: Soil contamination by metallic trace elements (MTEs) poses a significant environmental challenge, with far-reaching implications for human health and biodiversity. In this context, the exploration of biological methods for chelating MTEs has emerged as a promising, environmentally sustainable approach. Notably, certain metallophores, particularly pyoverdine, demonstrate effective scavenging properties, offering a viable solution. This study involved screening forty-five *Pseudomonas* isolates for their potential to extract these metals from contaminated soils. Additionally, we monitored the synthesis of various metabolites, including siderophores, *indole-3-acetic acid* (IAA), ammonia, hydrogen *cyanide* (HCN), and phosphate solubilization. The purified siderophore fraction was characterized using Fourier Transform Infrared Spectroscopy (FT-IR). Results indicated a notably higher level of siderophore production in *P. lactis*, *P. atacamensis*, and *Pseudomonas* sp. PS11. Particularly, the pyoverdine from *P. lactis* demonstrated a higher binding affinity for bromine, tin, rhodium, and lead. Our findings conclude that pyoverdine extracted from *P. atacamensis* exhibited an enhanced capacity for copper ion removal (49.63%), surpassing that of *P. lactis* (47.65%) and the control agents (EDTA and citric acid, ranging from 43.11% to 27.58%).

Key words: Soil contamination, metallic trace elements, pyoverdine, remove, PGPR.

1. INTRODUCTION

Environmental pollution has escalated significantly due to various human activities, including industrial operations, intensive agricultural practices, improper waste disposal, and other anthropogenic sources (Alengebawy et al., 2021). Trace metals, known for their inability to biodegrade, tendency to accumulate in environments (Jelea & Baciu, 2023; Hafsi et al., 2024), enduring presence, and harmful biological effects, pose significant risks to various ecosystems and living beings. The presence of these metals substantially impacts the physical and chemical characteristics of different natural matrices, including sediments, soil, and water. They bring about notable changes in soil attributes, including its pH, color, porosity, and overall chemical composition, and they also detrimentally affect the quality of water bodies (Ali et al., 2021). The extreme toxicity of MTEs, even at trace concentrations, and their inability to biodegrade like organic pollutants, pose a continual risk to life and the environment (Meliani & Bensoltane, 2016). Moreover, environmental pollution by MTEs not only incurs these repercussions but also heightens biosphere risks (Briffa et al., 2020). Consequently,

the Earth's ecosystems are increasingly unable to absorb and neutralize the growing concentration of heavy metals (HMs). The most eco-friendly approach to this problem lies in phytoremediation, especially utilizing Plant Growth Promoting Rhizobacteria (PGPR) agents, with growing awareness of their application in bioremediation.

Confronted with the issue of soil contamination by metallic trace elements, bioremediation stands out as an effective approach. This method utilizes the natural capabilities of microorganisms and plants to break down, eliminate, alter, or stabilize various environmental contaminants and waste materials. In this process, microorganisms play a crucial role, serving as biocatalysts through their enzymatic systems. These systems enable the progression of biochemical reactions that effectively break down and neutralize the targeted pollutants (Abatenh et al., 2017; Bala et al., 2022).

In this context, numerous metal-tolerant plant growth-promoting bacteria, isolated from metal-contaminated areas, are reported. These microbes enhance crop growth and yield by producing various growth-regulating biomolecules (Syed et al., 2023).

PGPR represents a distinct group of rhizobacteria known for their ability to enhance plant growth. They achieve this either directly or indirectly by colonizing the root systems of plants (Merdia et al., 2020). These beneficial bacteria stimulate plant growth by improving nutrient availability or inducing systemic resistance to suppress pathogen growth. Additionally, PGPR contribute to soil structure improvement and the mineralization of organic pollutants, thereby playing a crucial role in sustainable crop production (Hakim et al., 2021).

Under iron-deficient conditions, one effective strategy employed (PGPR) involves the production of siderophores. These are small molecules known for their specific chelating effect on the iron (III) cation, playing a pivotal role in iron acquisition (Chen et al., 2023). Recent evidence underscores the significance of using *Pseudomonas fluorescens*, a type of PGPR, as a viable alternative for such purposes (Singh et al., 2023).

Fluorescent *Pseudomonads*, in particular, are notable for producing fluorescent pyoverdines as their primary siderophore. To date, approximately 100 distinct pyoverdines have been identified (Grosse et al., 2023), garnering increasing attention for their potential in environmental bioremediation. Although traditionally recognized for their high specificity for iron, siderophores have also been reported to bind to a diverse array of metal and metalloid ions, such as Al^{3+}, Cr^{3+}, Ni^{2+}, Cu^{2+}, Zn^{2+}, Co^{2+}, Hg^{2+}, Pb^{2+}, and Cd^{2+} (Roskova et al., 2022; Xu et al., 2023). The chelation of metallic trace elements by siderophores not only reduces the toxicity of MTE ions but also enhances their availability in the rhizosphere, increases their uptake and accumulation by plants, and improves the effectiveness of phytoremediation (Zhang et al., 2023).

In this context, the current article aims to provide an eco-friendly alternative to chemical metal chelators in the bioremediation of soils polluted with MTEs. It evaluates the efficiency of bacterial siderophores and their applicability in washing contaminated soils.

2. MATERIALS AND METHODS

2.1. Isolation of rhizosphere bacteria resistant to heavy metals

2.1.1. Sampling

Samples of grapevine (*Vitis vinifera* L.) roots (rhizoplane and rhizosphere) were collected in sterile collection bags and transported to the laboratory. The sampling was carried out in November 2020 and March 2021, (Latitude: 35°54’ 42.53” N Longitude: 0° 16’34.94” E) Mostaganem, North West of Algeria.

2.2. Determination of the minimum inhibitory concentration by Microdilution method

Sterile 96-well microplates were utilized for this experiment. Initially, 100 µl of sterile Mueller-Hinton broth was accurately dispensed into each well of the microplate using a micropipette. Subsequently, 100 µl of MTEs solution at varying concentrations (6, 8, 10, 12, 14, and 16 mM) were added to the wells. To each well, 10 µl of a 0.5 McFarland bacterial suspension for each isolate was introduced. The microplate was then incubated at 30°C for 24 hours (Adhami et al., 2017). Cell viability was determined using triphenyl tetrazolium chloride (TTC), prepared at a concentration of 0.4 mg/ml in sterile distilled water and filtered through a 0.22 µm Millipore filter. A volume of 40 µl of this solution was added to each well. The plates underwent a secondary incubation at 30°C for 10-30 minutes. Cell viability was indicated by a color change to red in the presence of TTC (Varma et al., 2021).

2.3. Plant Growth-Promoting Parameters

2.3.1. Qualitative Phosphate solubilization

The phosphate solubilization activity of the isolates was assessed on Pikovskaya agar, which contains 5 g of tricalcium phosphate ($Ca_3(PO_4)_2$). Each plate was individually inoculated with bacteria

and incubated at 30°C for 7 days. Zones of clarity or solubilization around the colonies were observed to determine solubilization activity (Mehta & Nautiyal, 2001).

2.3.2. Quantitative evaluation in a liquid medium

The NBRIP liquid medium was utilized. Each 50 ml of this medium was inoculated with 1 ml of bacterial suspension from the respective isolates (OD_{620} = 0.08). The cultures were then incubated at 30°C for a duration of 7 days in a shaker incubator operating at 180 rpm. Following incubation, 5 ml from each culture was subjected to centrifugation at 4000 rpm for 30 minutes. The amount of soluble phosphate present in the supernatant was subsequently measured using the Vanadate-molybdate spectrophotometric technique (Hamoum et al., 2015).

For the determination of soluble phosphorus concentration, 1 ml of the supernatant was combined with 2.5 ml of Barton reagent in a 50 ml flask. This mixture was then diluted to 50 ml with distilled water. After allowing the mixture to stand for 10 minutes, the optical density was assessed at a wavelength of 430 nm using a SPECORD 210 Plus Analytica spectrophotometer. The concentration of soluble phosphorus in the sample was calculated using a regression equation derived from a pre-established calibration curve.

2.3.3. Production of indole acetic acid (IAA)

The production capacity of indole acetic acid (IAA) by the bacteria being studied was assessed in nutrient broth (NB). For this purpose, each 50 ml of NB, fortified with 0.01% D-tryptophan, received an inoculation of 1 ml of bacterial suspension, with an optical density (OD) at 620 nm of 0.08 (Kesaulya et al., 2015). This process was carried out both in the presence and absence of 5 mM $CuSO_4$. The cultures were then incubated for a duration of 4 days at 30°C, in dark conditions and under shaking at 180 rpm. Post-incubation, the bacterial cultures were subjected to centrifugation at 4000 rpm for 30 minutes. For assessing IAA production, 1 ml of the supernatant was combined with 4 ml of Salkowski's reagent, facilitating the formation of tris-(indole-3-acetic) iron (III) in correlation with the reaction. The levels of IAA were then determined using a regression equation derived from a previously established calibration curve.

2.3.4. Hydrogen cyanide production

The production of hydrogen cyanide (HCN) by bacterial isolates was evaluated using a nutrient agar medium enriched with 4.4 g/L glycine. A Whatman filter paper No. 1, saturated in a solution of 0.5% picric acid and 2% sodium carbonate, was positioned inside the lid of each agar plate. These plates were then securely sealed with parafilm and incubated at a temperature of 28±2°C for a period of 4 days. For control purposes, some plates were not inoculated with any bacterial isolates. The indication of HCN production was determined by observing a color shift from yellow to orange on the filter paper (Ponmurugan et al., 2011).

2.3.5. Ammonia production

The production of ammonia by the bacterial isolates was evaluated using the methodology outlined by Cappuccino & Sherman (1992). Bacterial cultures grown overnight were introduced into 10 ml of peptone broth and then incubated at 30°C for 48 hours on a shaker operating at 120 rpm. Following the incubation period, 0.5 ml of Nessler's reagent was added to each sample. The presence of ammonia was indicated by a change in color within the samples, varying from faint yellow to dark brown.

2.3.6. Siderophore production

The production of siderophores by bacterial isolates was assessed utilizing the methodology developed by Schwyn & Neilands (1987). For this purpose, the bacteria were cultured on Chrome Azurol S (CAS) agar medium. These plates were then incubated in dark conditions at a temperature of 30°C for a duration of 5 days. The emergence of a yellow-orange halo surrounding the bacterial colonies served as an indicator of positive siderophore production (Kamaruzzaman et al., 2020).

2.3.7. Quantitative Siderophore production assay

Siderophore production by *Pseudomonas* isolates was quantitatively assayed in succinate medium, as per the protocol outlined by Schwyn & Neilands (1987). Each isolate was independently cultivated in a 500-ml flask containing 100 ml of succinate medium, maintained at 30 °C, and agitated at 120 rpm for a period of 48 hours. Following incubation, the cell density of each culture was measured at 620 nm using a UV-visible spectrophotometer. Siderophores in the cell-free supernatant, which was obtained after centrifugation (20 minutes at 4,000 g), were detected and quantified using the Chromium Azurol Sulphonate (CAS) assay. The concentration of siderophores was calculated as a percentage of siderophore units using the formula: Siderophore Unit Percentage = (Ar - As) / Ar × 100, where Ar represents the reference absorbance at 630

nm (CAS reagent) and As denotes the sample absorbance at 630 nm (Kejela et al., 2017).

2.4. Extraction and estimation of siderophore

After 48 hours of incubation, 1000 ml of the succinate medium, inoculated with the bacterial cultures, was centrifuged at 4000 g for 20 minutes. The resulting cell-free supernatant had its pH adjusted to 2.0 using concentrated HCl, and was then left to stand overnight at 4°C. According to the procedure outlined by Schwyn & Neilands (1987), this supernatant was then subjected to extraction using ethyl acetate (v/v). After the extraction process, the ethyl acetate layer was evaporated to yield the siderophore.

2.4.1. Purification of siderophore

The extracted siderophore was purified using an XAD-4 resin adsorption column. The column preparation involved suspending approximately 30 g of XAD-4 in dH2O and allowing the mixture to stand at room temperature overnight to fully absorb the water. After packing the column with the prepared XAD-4, it was equilibrated with double-distilled water (ddH2O) until a conductivity of 2 µs cm^{-1} was achieved. The crude siderophore extract was then introduced into the column. Elution was performed using approximately 250 ml of methanol, collecting five 50 ml fractions. The purification process of the siderophore was monitored at each step using the liquid CAS assay (Nithyapriya et al., 2021).

2.4.2. Characterization of siderophore by Fourier Transform Infra-Red (FT-IR)

The purified siderophore fraction was prepared for Fourier Transform Infrared (FT-IR) analysis, which was conducted in the range of 4000–400 cm^{-1}. The infrared spectrum wavelengths were identified based on their respective functional groups.

2.5. Soil Sampling and Preparation

Soil samples were gathered from the surface layer, extending to a depth of 0-30 cm. In preparation for analysis, these samples were air-dried, finely ground, and then passed through a 2 mm mesh sieve. This process was undertaken to eliminate any debris and stones, thereby ensuring the samples were suitable for subsequent analytical procedures.

2.5.1. Batch Washing Studies

The effectiveness of siderophore, EDTA (a chemical chelating agent at 0.01M concentration), and citric acid (an organic chelating agent also at 0.01M) in extracting metallic trace element (MTE) ions from soil was evaluated on a batch scale. For this purpose, soil samples (Table 1) were artificially spiked with 5 g/kg of $CuSO_4$ (Sayyed et al., 2013). The batch washing tests involved the use of sealed 250 mL glass flasks, which were agitated at 180 rpm on a mechanical shaker. After a period of 24 hours, the supernatant was separated from the soil sediment through centrifugation at 4000 rpm for 15 minutes. The MTE content in the supernatant was then measured using an X-ray fluorescence spectrometer, XEPOS P. The percentage of MTEs removed from the solution was calculated using the following equation: % Adsorption= $Co - Ce / Co \times 100$

Table 1. Physical and chemical properties of the examined soil.

Parameter	**Unit**	**Norme**	**Value**
pH	-	ISO 10390	7.6
EC	mS/cm	ISO 11265	0.07
R.M	%	AFNOR NF X 31-102 (1992)	75.08
O.M.	%	-	1.14
Carb	%	-	0.22
N_2	-	ISO 11261	0.049
P	Mg/l	-	0.22
K	Mg/l	-	6.16
Ca	Mg/l	-	62
Mg	Mg/l	-	3.66
Na	Mg/l	-	10.35
Particle size distribution			
Sand		68	
Clay		12	
Silt		20	

Where *Co* is the initial concentration of heavy metal and *Ce* is the final concentration of MTEs (Mahmoud et al., 2015; Zhao et al., 2019).

Genetic identification of Pseudomonas strains

The genetic identification of *Pseudomonas* strains PO22, R2P30, and PS11, which exhibited higher siderophore production, was conducted by extracting total DNA using the protocol provided by Macherey-Nagel, Germany. The entire 16S rRNA gene from these isolates was amplified with universal primers: Start (forward) 5′ AGAGTTTGATCMTGGCTCAG 3′ and End (reverse) 5′ TACGGYACCTTGTTACGACTT 3′. Following amplification, the 16S rRNA genes were purified and sequenced utilizing the enzymatic chain terminator technique with a BigDye v3.1 kit from Applied Biosystems. The resulting nucleotide sequences were then aligned with *Pseudomonad* 16S rRNA gene sequences from the GenBank database (http://www.ncbi.nlm.nih.gov). These sequences were deposited and compared to those in the GenBank database using the NCBI BLAST Program. Phylogenetic trees were constructed using the MEGA version 11 software, applying the Neighbor-Joining method.

2.6. Statistical analyses

For statistical analysis, SPSS Statistics 26 software was employed. P-values were determined using the Kruskal-Wallis nonparametric test, followed by Dunn's post hoc analysis to ascertain statistical significance, which was set at $P < 0.05$. Additionally, Principal Component Analysis (PCA) was performed using STATISTICA 7.0 software.

3. RESULTS AND DISCUSSION

3.1. Molecular Identification of Bacterial Isolates

Pseudomonas isolates PO22, R2P30, and PS11, noted for their superior siderophore production in this study, were genetically identified via sequencing of their 16S rRNA genes. This identification process included a BLAST search at the National Center for Biotechnology Information website (http://www.ncbi.nlm.nih.gov). Further analysis using the EzBioCloud online tool, which encompassed both 16S rRNA and BLAST results, indicated that isolate PO22 closely resembled various strains of *P. atacamensis*, exhibiting 100% homology. Similarly, *Pseudomonas* isolate R2P30 was identified as *P. lactis*, showing a 99.28% homology, while isolate PS11 was classified as *Pseudomonas* sp., with a homology percentage of 99.14%. These findings are referenced under the accession numbers OQ726322, OQ726323, and OQ726353.

1A phylogenetic tree (Figure 1) was constructed to depict the relationships between fluorescent *Pseudomonas* isolates F2, F7, and F8, along with other well-established members of the *Pseudomonas* genus. This tree was generated using the UPGMA (Unweighted Pair Group Method with Arithmetic Mean) method within MEGA version 11. It provides a visual representation of the genetic connections among these isolates, offering insights into their evolutionary relationships.

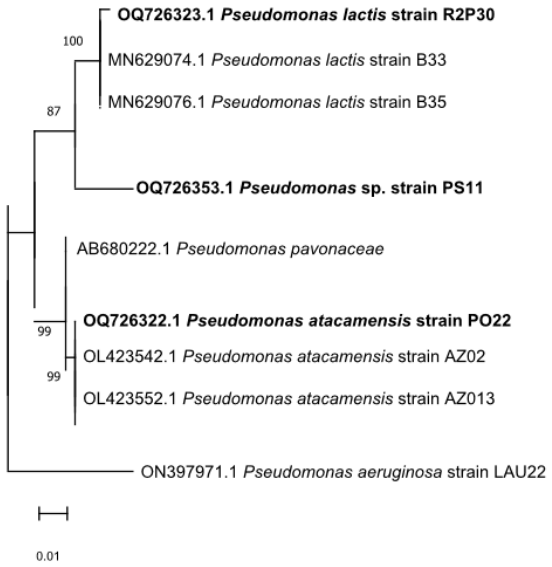

Figure 1. Phylogenetic tree illustrating the relationship between strains R2P30, PO22, and PS11 and the most closely related *Pseudomonas* sp. species.

3.2. Determination of Minimum Inhibitory Concentration (MIC)

Upon testing 45 distinct *Pseudomonas* isolates for copper sensitivity, the minimum inhibitory concentration (MIC) for MTEs was established at 12 mM, following the addition of TTC. These isolates exhibited a high copper tolerance, ranging from 6 mM to 12 mM. Rajbanshi (2008) reported that all isolates displayed significant resistance to 300 µg/ml of copper. In contrast, Benhalima et al., (2019) found that 400 µg/ml of copper inhibited 25% of their *Pseudomonas* isolates. Additionally, Singh et al. (2010) indicated that the MIC of copper in tested *Pseudomonas* strains varied between 180 and 300 µg/ml.

3.2.1. Indol Acid Acetic production

Testing of 45 rhizosphere isolates of *Pseudomonas* for IAA production revealed that 60%

were capable of producing IAA, with quantities ranging from 144 to 577.14 µg/mL. The highest production was observed in *P. lactis* (R2P30) with 428.19 µg/ml, followed by *P. atacamensis* (PO22) with 342.28 µg/ml and *Pseudomonas* sp. (PS11) with 165.47 µg/ml. The presence of copper significantly affected IAA production ($p \leq 0.05$), causing a decrease ranging from 7.3 to 48.9% in most isolates.

3.2.2. HCN and ammonia production

Among the 45 isolates tested, 20 (44.4%) demonstrated HCN production after 4 days of incubation (Figure 2). Additionally, a significant majority, 41 isolates (91%), exhibited the ability to produce ammonia. Various bacterial taxa, including Bacillus sp. and *Pseudomonas* sp., are known for their HCN production in stressful environments. Notably, the ammonia production by these microbial strains was unaffected by different doses of Cd (Syed et al., 2023). Previous studies have indicated that the presence of metals other than iron in the bacterial environment can influence the production of siderophores (Schalk et al., 2020).

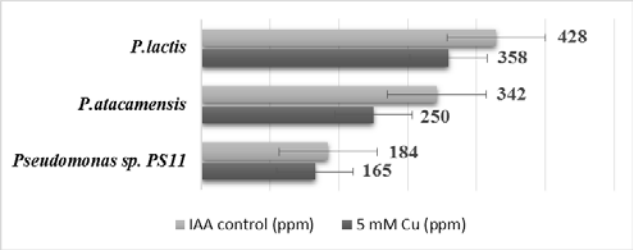

Figure 2. Indol acetic acid specific production

3.2.3. Phosphore solubilization

Phosphate solubilization capabilities were observed in 84% of the bacteria, as evidenced by the formation of transparent zones on Pikovskaya medium (Figure 2). The quantities of organic acids produced during solubilization in NBRIP medium varied, ranging from 35 to 840 µg/ml. Plant growth-promoting rhizobacteria (PGPR) enhance plant growth through mechanisms such as phosphate solubilization, siderophore production, biological nitrogen fixation, quorum sensing signal interference, biofilm formation inhibition, and phytohormone production (Mushtaq et al., 2022). They also assist plant growth under MTEs stress by producing chelating agents, promoting an elongated root system, inducing resistance to abiotic stress, and increasing the availability of essential nutrients (Zhu et al., 2023).

3.3. Siderophores production

All bacterial isolates underwent evaluations to determine their siderophore production capabilities, employing both qualitative and quantitative methods. In the qualitative assessment on CAS agar plates, siderophore-producing isolates displayed the formation of a yellow to orange zone surrounding their colonies, indicative of iron chelation. To validate these findings, quantitative measurements of siderophore production were conducted in liquid cultures. Among the isolates, *P. lactis* (R2P30), *P. atacamensis* (PO22), and *Pseudomonas* sp. (PS11) demonstrated the highest levels of siderophore production, with percentages of 67.69%, 66.53%, and 56.86%, respectively, in succinic medium.

3.3.1. Characterization of Purified Pyoverdine by FT-IR

(FT-IR) spectroscopy results of purified siderophores are detailed in Figure 3, highlighting various peaks detected at different wavenumbers (cm^{-1}). The spectrum shows a broad band at 3375 cm^{-1}, indicative of the presence of an OH group of alcohol (R-OH) and the elongation of the N-H group, characteristic of secondary amides. Another significant band, observed at 2958 cm^{-1}, corresponds to the free OH function, typically associated with carboxylic acid (R-COOH), with the C=O bond denoting the presence of the carbonyl group. Additionally, the absorption band observed at 2300 cm^{-1} can be associated with the presence of the benzoic ring, whereas the band detected at 1750 cm^{-1} is indicative of the C=O group.

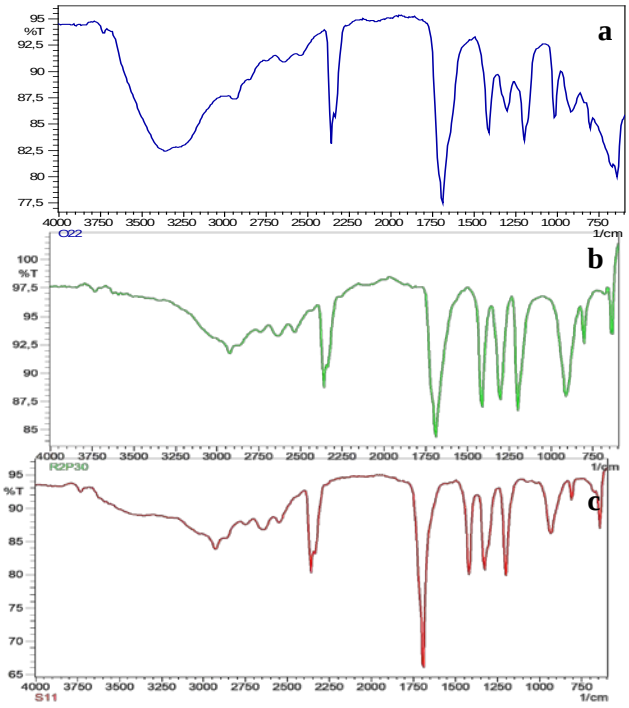

Figure 3. FT-IR spectra of pyoverdine of (a) *P. atacamensis*, (b) *P. lactis*, and (c) *Pseudomonas sp.*PS11.

The spectrum also reveals bands between 1208 and 1450 cm-1, which are characteristic of the elongation of the aromatic C=C group. Notably, a band located at 1333 cm-1 is ascribed to the elongation of the C=O group. A second, thinner band at 1041 cm^{-1} corresponds to the C-O and C=N bonds. Furthermore, a band beyond 980 cm^{-1} is associated with the N-H bond. These findings are consistent with the presence of pyoverdine, as also reported by Tank et al., (2012) and Shainy et al., (2016). The detection of bands between 1208 and 1450 cm^{-1}, attributed to the elongation of the aromatic C=C group, further corroborates this identification. The characterization of the purified siderophore extract through FT-IR spectroscopy thus reveals a composition similar to pyoverdine, aligning with previous studies in the field.

3.3.2. Washing soil solution

The study revealed that siderophores, EDTA, and citric acid solutions effectively extracted MTEs from contaminated soil, surpassing the control conditions (Figure 4). Statistical analysis using the Kruskal–Wallis test, with a significant p-value (<0.05), confirmed notable differences in mean removals of MTEs from water among these groups. A comparative assessment of heavy metal (HM) removal efficiencies revealed no significant distinction among the EDTA solutions ($p < 0.05$). However, *P. lactis* pyoverdine was found to be more effective in removing MTEs from contaminated soil than *P. atacamensis*, *Pseudomonas* sp. PS11, and citric acid ($p > 0.05$).

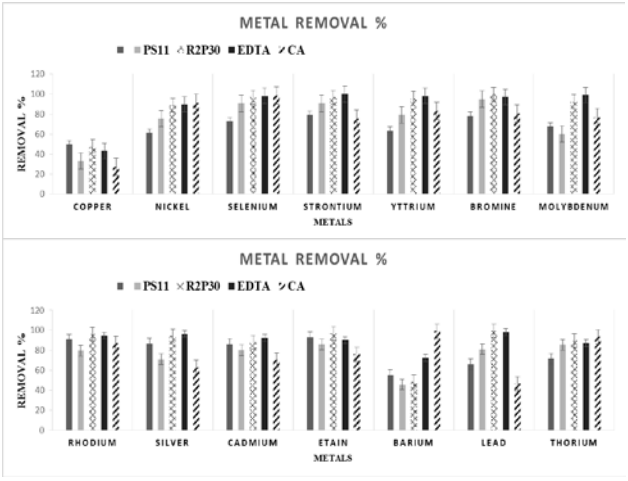

Figure 4. Extraction of MTEs from soil with different solution siderophore, EDTA, and citric acid after 24 hours of agitation.

P. atacamensis pyoverdine exhibited a superior capacity to remove copper ions (49.63%), followed by *P. lactis* (47.65%), outperforming EDTA (43.11%) and citric acid (CA) (27.58%). Interestingly, P. *lactis* pyoverdine also showed a higher binding affinity for bromine, tin, rhodium, and lead than EDTA, with a similar affinity for nickel (89%).

Our findings demonstrate that *P. lactis* pyoverdine is effective in removing MTEs from contaminated soil, a capability not paralleled by *P. atacamensis*, *Pseudomonas* sp. PS11, or citric acid ($p > 0.05$). Notably, *P. atacamensis* pyoverdine shows a superior ability to remove copper ions (49.63%), followed closely by P. *lactis* (47.65%), and significantly outperforms both EDTA (43.11%) and citric acid (CA) (27.58%). Additionally, *P. lactis* pyoverdine exhibits a higher binding affinity for bromine, tin, rhodium, and lead compared to EDTA, with a comparable affinity for nickel (89%).

Siderophores are primarily specific to ferric ions but also have the capability to bind and chelate other MTEs due to their high metal-siderophore stability constants. Siderophores are known to complex with various metal ions besides iron (Patel et al., 2016).

Pyoverdines, a type of siderophore, are particularly adept at chelating a range of metals other than iron (Schalk et al., 2020). When MTEs bind to free siderophores, they hinder the chelation of iron ions, reducing the amount of accessible iron. This, in turn, stimulates the synthesis of more siderophores, aiding bacterial or plant survival and offering partial protection from the toxicity of MTEs (Zhang et al., 2023).

The binding affinity of siderophores to various metal ions is affected by the structural features of their functional groups, as well as the size and charge of cations. Although sulfur and nitrogen-based metal-binding motifs in siderophores exhibit strong affinities for divalent ions like Cu^{2+}, Zn^{2+}, and Ni^{2+}, the primary functional groups, which are oxygen-containing hydroxamate, catecholate, and carboxylate residues, tend to have a preference for trivalent ions over divalent ones (Hofmann et al., 2021).

3.4. Multivariate analysis using Principal component analysis (PCA)

(PCA) plays a crucial role in multivariate analysis by emphasizing variations in the removal of heavy metals (HMs) through the examination of correlation matrices and varimax rotation. The initial two principal components (PCs a and b), illustrated in Figure 5, collectively explain a significant portion of 80.31% of the total variance.

The first axis, representing 49.86% of the variance, is strongly positively correlated with

CU_AIA (R = 0.93) and AIA (R = 0.88), and to a lesser extent with PO4 (R = 0.59). This axis characterizes strains R2P10, CA, and R2P29 positively, while strains PO15 and PO38 are characterized negatively. The second axis, accounting for 30.55% of the variance, shows a positive correlation with SIDEROPH (R = 0.89) for strains R2P30, PO22, and PS11, and a negative correlation with PO4 (R = -0.59), primarily characterized by observations of strains PO6, PO12, PO23, and PO10.

The last set of PCs (c and d), as shown in Figure 5, contributes 86.07% of the information. The first axis of this set is strongly positively correlated with several metals, including lead (R = 0.95), strontium (R = 0.91), silver (R = 0.91), and others, mainly characterizing R2P30 and EDTA, while showing a strong negative correlation with barium (R = -0.44), which is predominant in CA. The second axis is positively correlated with thorium (R = 0.97), selenium (R = 0.95), nickel (R = 0.94), and other elements, primarily characterizing CA.

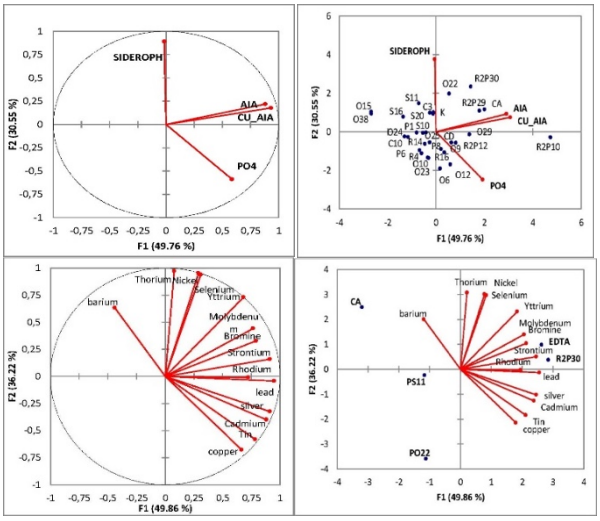

Figure 5. The two PCA results, showing clear separation between factors (siderophores, AIA, PO4) and variables (isolates). AIA, AIA-Cu, and PO4 are positioned on one side, while siderophore is on the opposite side of the two principal components (PCs a and b). A different grouping of metals is observed for the second set of PCs (c and d), where barium shows a marked separation from other metals.

To further categorize HM removal groups, Hierarchical Cluster Analysis (HCA) was employed. The dendrogram, presented in Figure 6, is divided into two subclusters. The first group consists of samples predominantly containing molybdenum and tin, while the second group is characterized by barium and selenium. This clustering illustrates the similarities and differences in the removal of MTEs by various treatments, indicating that R2P30, EDTA, and PS11 exhibit significant similarities in their ability to remove HMs.

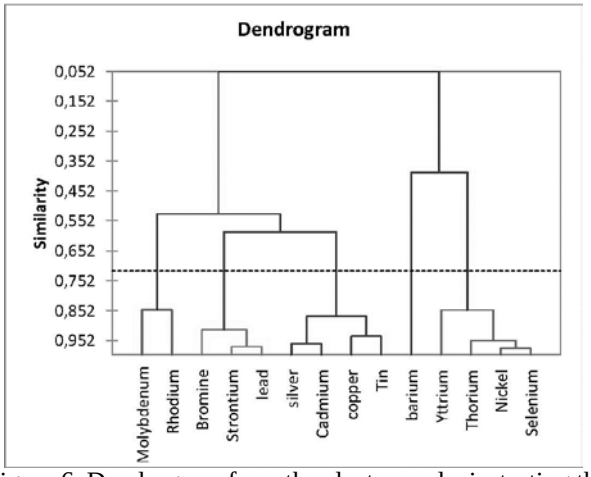

Figure 6. Dendrogram from the cluster analysis, testing the similarity level in the removal of MTEs. It highlights the proximity of R2P30, EDTA, and PS11 in their efficacy in removing HMs.

4. CONCLUSION

The findings of this research demonstrate that *Pseudomonas* siderophores are capable of producing and releasing a broad spectrum of bioactive compounds, underscoring their significant potential in the bioremediation of metallic trace elements (MTEs). Notably, the chelation efficacy of *Pseudomonas* pyoverdine is comparable to that of EDTA and citric acid, emphasizing its viability as an eco-friendly alternative for the remediation of MTEs-contaminated soils. This highlights the promise of using such biological agents in environmentally sustainable soil decontamination strategies.

Acknowledgement

We would like to thank all those who contributed to this article's completion. Special thanks to Dr. Yeşim DAĞLIOĞLU for their valuable input. We also acknowledge the support from Higher school of agronomy Mostaganem, Algeria for providing resources.

REFERENCES

Abatenh, E., Gizaw, B., Tsegaye, Z., & Wassie, M., 2017. *The role of microorganisms in bioremediation-A review.* Open Journal of Environmental Biology, 2(1), 038-046.

Adhami, E., Aghaei, S., & Zolfaghari, M. R., 2017. *Evaluation of heavy metals resistance in biofilm cells of native Rhodococcus spp. isolated from soil.* Archives of Hygiene Sciences, 6(3), 235-243.

Alengebawy, A., Abdelkhalek, S. T., Qureshi, S. R., & Wang, M. Q., 2021. *Heavy metals and pesticides toxicity in agricultural soil and plants: Ecological*

risks and human health implications. Toxics, 9(3), 42.

Ali, M. M., Hossain, D., Khan, M. S., Begum, M., Osman, M. H., Nazal, M. K., & Zhao, H., 2021. *Environmental pollution with heavy metals, A public health concern* (pp. 1-20). IntechOpen.

Bala, S., Garg, D., Thirumalesh, B. V., Sharma, M., Sridhar, K., Inbaraj, B. S., & Tripathi, M., 2022. *Recent strategies for bioremediation of emerging pollutants: A review for a green and sustainable environment.* Toxics, 10(8), 484.

Benhalima, L., Amri, S., Bensouilah, M., & Ouzrout, R., 2019. *Antibacterial effect of copper sulfate against multi-drug resistant nosocomial pathogens isolated from clinical samples.* Pakistan Journal of Medical Sciences, 35(5), 1322.

Briffa, J., Sinagra, E., & Blundell, R., 2020. *Heavy metal pollution in the environment and their toxicological effects on humans.* Heliyon, 6(9), e04691.

Cappuccino, J. G., & Sherman, N., 1992. *Biochemical activities of microorganisms. Microbiology, A Laboratory Manual.* The Benjamin/Cummings Publishing Co. California, USA, 76.

Chen, J., Sun, Z., Jin, J., Wang, F., Yang, Q., Yu, H., ... & Wang, Y., 2023. *Role of siderophore in Pseudomonas fluorescens biofilm formation and spoilage potential function.* Food Microbiology, 109, 104151.

Grosse, C., Brandt, N., Van Antwerpen, P., Wintjens, R., & Matthijs, S., 2023. *Two new siderophores produced by Pseudomonas sp. NCIMB 10586: The anti-oomycete non-ribosomal peptide synthetase-dependent mupirochelin and the NRPS-independent triabactin.* Frontiers in microbiology, 14.

Hafsi, A., Bourefis, A., Kessasra, F. & Boushaba, A., 2024. *Environmental assessment of pollution in an industrial environment using heavy metal pollution indices and stable isotopes, case study of the industrial zone of skikda, north-east algeria.* Carpathian journal of earth and environmental sciences, 19(1), 33-50

Hakim, S., Naqqash, T., Nawaz, M. S., Laraib, I., Siddique, M. J., Zia, R., ... & Imran, A., 2021. *Rhizosphere engineering with plant growth-promoting microorganisms for agriculture and ecological sustainability.* Frontiers in Sustainable Food Systems, 5, 617157.

Hamoum, H., Bouznad, A., Mekhaldi, A., & Djibaoui, R,. 2015. *Screening for PGP Activities of Diazotrophic Bacteria Isolated from Saline Soil and their Effect on Maize Growth under Saline Stress.* Journal of Pure and Applied Microbiology.

Hofmann, M., Heine, T., Malik, L., Hofmann, S., Joffroy, K., Senges, C. H. R., ... & Tischler, D., 2021. *Screening for microbial metal-chelating siderophores for the removal of metal ions from solutions.* Microorganisms, 9(1), 111.

Kamaruzzaman, M. A., Abdullah, S. R. S., Hasan, H. A., Hassan, M., Othman, A. R., & Idris, M., 2020. *Characterisation of Pb-resistant plant growth-promoting rhizobacteria (PGPR) from Scirpus grossus.* Biocatalysis and Agricultural Biotechnology, 23, 101456.

Jelea, O. C., & Baciu, C., 2023. *Effects of heavy metals, contained in flotation tailings, on plants used in revegetation.* Carpathian journal of earth and environmental sciences, 18(1), 89-103.

Kejela, T., Thakkar, V. R., & Patel, R. R., 2017. *A novel strain of Pseudomonas inhibits Colletotrichum gloeosporioides and Fusarium oxysporum infections and promotes germination of coffee.* Rhizosphere, 4, 9-15. **Kesaulya, H., Zakaria, B., & Syaiful, S. A.,** 2015. *Isolation and physiological characterization of PGPR from potato plant rhizosphere in medium land of Buru Island.* Procedia Food Science, 3, 190-199.

Mahmoud, A. M., Ibrahim, F. A., Shaban, S. A., & Youssef, N. A., 2015. *Adsorption of heavy metal ion from aqueous solution by nickel oxide nano catalyst prepared by different methods.* Egyptian Journal of Petroleum, 24(1), 27-35.

Mehta, S., & Nautiyal, C. S., 2001. *An efficient method for qualitative screening of phosphate-solubilizing bacteria.* Current microbiology, 43, 51-56.

Merdia, B., Rokaia, B. M., Kheira, F., & Asmaa, B., 2020. *Biological control by Plant Growth Promoting Rhizobacteria*. ALGERIAN JOURNAL OF BIOSCEINCES, 1(02), 30-36.

Meliani, A., & Bensoltane, A., 2016. *Biofilm-mediated heavy metals bioremediation in PGPR Pseudomonas*. J Bioremediat Biodegrad, 7(2).

Mushtaq, Z., Liaquat, M., Nazir, A., Liaquat, R., Iftikhar, H., Anwar, W., & Itrat, N., 2022. *Potential of plant growth promoting rhizobacteria to mitigate chromium contamination.* Environmental Technology & Innovation, 28, 102826.

Nithyapriya, S., Lalitha, S., Sayyed, R. Z., Reddy, M. S., Dailin, D. J., El Enshasy, H. A., & Herlambang, S., 2021. *Production, purification, and characterization of bacillibactin siderophore of Bacillus subtilis and its application for improvement in plant growth and oil content in sesame.* Sustainability, 13(10), 5394.

Patel PR., Shaikh SS., & Sayyed, RZ., 2016. *Dynamism of PGPR in bioremediation and plant growth promotion in heavy metal contaminated soil.* Indian Journal of Experimental Biology Vol. 54, pp. 286-290

Ponmurugan, P., Manjukarunambika, K., & Reddy, M. S., 2011. *In vitro studies on efficacy of Pseudomonas spp. for plant growth promoting traits and biocontrol of diseases in tea plants.* Plant Growth-Promoting Rhizobacteria (PGPR) for Sustainable Agriculture, 166.

Rajbanshi, A., 2008. *Study on Heavy Metal Resistant Bacteria in Guheswori Sewage Treatment Plant.* Our nature, 6(1).

Roskova, Z., Skarohlid, R., & McGachy, L., 2022. *Siderophores: an alternative bioremediation*

strategy?. Science of The Total Environment, 153144.

Sayyed, R. Z., Patel, P. R., & Reddy, M. S., 2013. *Role of PGPR in bioremediation of heavy metal ions and plant growth-promotion of wheat and peanut grown in heavy metal contaminated soil. In Recent advances in biofertilizers and biofungicides (PGPR) for sustainable agriculture*. Proceedings of 3rd Asian Conference on Plant Growth-Promoting Rhizobacteria (PGPR) and other Microbials, Manila, Philippines, 21-24 April, 2013 (pp. 112-128). Asian PGPR Society for Sustainable Agriculture.

Schalk, I. J., Rigouin, C., & Godet, J., 2020. *An overview of siderophore biosynthesis among fluorescent Pseudomonads and new insights into their complex cellular organization.* Environmental Microbiology, 22(4), 1447-1466.

Schwyn, B., & Neilands, J. B., 1987. *Universal chemical assay for the detection and determination of siderophores.* Analytical biochemistry, 160(1), 47-56.

Shainy, K. M., Rugmini Ammal, P., Unni, K. N., Benjamin, S., & Joseph, A., 2016. *Surface interaction and corrosion inhibition of mild steel in hydrochloric acid using pyoverdine, an eco-friendly bio-molecule.* Journal of Bio-and Tribo-Corrosion, 2, 1-12.

Singh, P., Singh, R. K., Li, H. B., Guo, D. J., Sharma, A., Verma, K. K., ... & Li, Y. R., 2023. *Nitrogen fixation and phytohormone stimulation of sugarcane plant through plant growth promoting diazotrophic Pseudomonas.* Biotechnology and Genetic Engineering Reviews, 1-21.

Singh, V., Chauhan, P. K., Kanta, R., Dhewa, T., & Kumar, V., 2010. *Isolation and characterization of Pseudomonas resistant to heavy metals contaminants.* International Journal of Pharmaceutical Sciences Review and Research, 3(2), 164-167.

Syed, A., Elgorban, A. M., Bahkali, A. H., Eswaramoorthy, R., Iqbal, R. K., & Danish, S., 2023. *Metal-tolerant and siderophore producing Pseudomonas fluorescence and Trichoderma spp. improved the growth, biochemical features and yield attributes of chickpea by lowering Cd uptake.* Scientific Reports, 13(1), 4471.

Tank, N., Rajendran, N., Patel, B., & Saraf, M., 2012. *Evaluation and biochemical characterization of a distinctive pyoverdin from a Pseudomonas isolated from chickpea rhizosphere.* Brazilian Journal of Microbiology, 43, 639-648.

Varma, A., Gemeda, H. B., McNulty, M. J., McDonald, K. A., Nandi, S., & Knipe, J. M., 2021. *Bioprinting transgenic plant cells for production of a recombinant biodefense agent.* bioRxiv

Xu, Y. C., Li, N., Yan, X., & Zou, H. X., 2023. DFT-based Analysis of Siderophore-Metal Ion Interaction for Efficient Heavy Metal Remediation.

Zhang, S., Deng, Z., Borham, A., Ma, Y., Wang, Y., Hu, J., ... & Bohu, T., 2023. *Significance of Soil Siderophore-Producing Bacteria in Evaluation and Elevation of Crop Yield.* Horticulturae, 9(3), 370.

Zhao, J., Shen, X. J., Domene, X., Alcañiz, J. M., Liao, X., & Palet, C., 2019. *Comparison of biochars derived from different types of feedstock and their potential for heavy metal removal in multiple-metal solutions.* Scientific Reports, 9(1), 9869.

Zhu, Y., Wang, Y., He, X., Li, B., & Du, S. (2023). *Plant growth-promoting rhizobacteria: A good companion for heavy metal phytoremediation*. Chemosphere, 139475.

Received at:05. 02. 2024
Revised at: 17. 02. 2024
Accepted for publication at: 19. 02. 2024
Published online at: 23. 02. 2024